Sensors and Materials, Vol. 37, No. 3 (2025) 955–964
MYU Tokyo

S & M 3968

Direct Detection of Polystyrene Nanoplastics in Water Using High-sensitivity Surface-enhanced Raman Scattering with Ag Nanoarray Substrates

Yifeng Guo,[1†] Yu Wang,[2†] Limin Huang,[3] Hongqi Li,[4]
Xiaohong Wang,[4] Xiaobo Jia,[4] Zhaoxu Li,[5] and Yansheng Liu[4*]

[1]School of Electrical and Information Engineering, Chengdu University,
2025 Chengluo Avenue, Chengdu, Sichuan 610106, China
[2]School of Business, Chengdu University, 2025 Chengluo Avenue, Chengdu, Sichuan 610106, China
[3]School of Mechanical Engineering, Chengdu University, 2025 Chengluo Avenue, Chengdu, Sichuan 610106, China
[4]School of Electronic Engineering, Guangxi University of Science and Technology,
No. 2, Wenchang Road, Liuzhou City, Guangxi 545006, China
[5]The Second People's Hospital of Guangxi Zhuang Autonomous Region,
No. 2, Diecai Road, Diecai District, Guilin City, Guangxi 541001, China

(Received November 12, 2024; accepted February 12, 2025)

Keywords: surface-enhanced Raman scattering (SERS), PS nanoplastics, Ag arrays

Nanoplastics generated from plastic materials have been of utmost concern to human and ecosystem health. Because of their tiny size, nanoplastics can easily penetrate biological barriers and enter cells, resulting in unknown diseases. Although there is growing interest in detecting nanoplastics, and many techniques have been utilized to detect nanoplastics, a fast, easy, and reliable method is still required. Hence, an efficient method based on surface-enhanced Raman scattering (SERS) with periodic Ag nanoarray (AgNA) substrates shows promising potential in detecting polystyrene nanoplastics (PSNPs) with high sensitivity. By thermally evaporating Ag onto periodic anodic aluminum oxide (AAO) templates, the AgNA with high SERS performance is fabricated. The SERS performance of the AgNA is studied by changing its height. By directly drop-casting PSNPs onto the AgNA, the limit of detection (LOD) for PS becomes 10 μg/mL. Moreover, the AgNA is applied to detect PSNPs under different real water conditions with good recovery rates. Thus, this easily fabricated and highly sensitive SERS substrate provides a fast, efficient, and practical way to detect PSNPs in aqueous media.

1. Introduction

Plastics play a very important role in our life. Owing to their unique properties such as affordability, durability, and lightweight, plastics have been widely used as industrial materials and fabricated into machine casings, bottles, bowls, plates, and cloth. Large pieces of wasted plastics can decompose into small particles with diameters ranging from micrometers to nanometers under photodegradation, oxidation, hydrolysis, and mechanical crushing.(1) These

*Corresponding author: e-mail: Yansheng.liu@gxust.edu.cn
†These authors contributed equally to this work and should be considered co-first authors.
https://doi.org/10.18494/SAM5477

ISSN 0914-4935
https://myukk.org/

microsize and nanosize particles as emerging environmental contaminants are of utmost concern owing to their ubiquitous presence and threat. Plastic particles have been found in water systems,[2] oceans,[3] soil,[3] food,[4] and organisms.[5] It has been reported that plastic particles can accumulate in the human body through the dietary intake of food, water, and air. Plastics can enter into the bloodstream and urine, which brings a great potential risk of illness. Although the toxicity and disease-causing properties of plastic particles are debatable, a fast, easily operated, and accurate method for detecting plastic particles is still important to reduce the potential risk of plastic particles to human health.

The diameter of nanoplastic particles (NPPs) is below 1 μm. Mass spectrometry, pyrolysis gas chromatography–mass spectrometry,[6] conventional Raman spectroscopy,[7–9] Fourier-transform infrared spectroscopy,[10,11] thermal desorption proton-transfer-reaction mass spectrometry,[12] and inductively coupled plasma mass spectrometry[13,14] are widely applied to detect MPPs/NPPs. These technologies exhibit high sensitivity and low limit of detection (LOD), but the sample needs to be purified and degraded into small molecules using the proper solvent. This makes the detection process complex and inconvenient in comparison with direct detection methods without pretreatment.

Raman scattering is a method of identifying the fingerprint of molecules. Raman spectroscopy as an easily operated and fast technique can be applied to varying scenarios with good accuracy. Additionally, owing to the linear relationship between Raman scattering intensity and the concentration of target materials, Raman scattering can be used for quantitative analysis. However, the weak signal of Raman spectroscopy restricts its application to NPPs with low concentrations. Surface-enhanced Raman scattering (SERS) is a method of prominently enhancing Raman scattering signals using SERS substrates. As a surface technique, SERS exhibits several advantages such as being fast and convenient and having high sensitivity and a single-molecule detection limit.[15,16] By applying metallic nanostructures, the SERS intensity can be significantly improved. The commercially available periodic Klarite substrate,[17] Ag core embedded Au film (Ag@AuFilm),[18] and porous AAO/MoS_2/Ag array[19] have been applied to detect PS NPPs with nanoscale diameters, and they show good detection performance.

The enhancement mechanisms of SERS involve both the chemical mechanism (CM) and the electromagnetic mechanism (EM). CM arises from the charge transfer between metal nanoparticles (NPs) and molecules, whereas EM is driven by the resonance of the surface plasmon excitations (SPR) of metallic nanostructures, which significantly amplifies the SERS signal. Typically, these two mechanisms work in tandem to enhance the SERS signal.[16] For optimal SERS performance, self-assembled or aggregated Au or Ag nanoparticles are the most widely used substrates.[20,21] While these structures are relatively easy to fabricate, their inhomogeneity can negatively affect the SERS performance, particularly in quantitative analytical applications. Their random aggregation often results in broad plasmon resonance absorption, leading to poor SERS enhancement. In contrast, periodically ordered nanomaterials offer uniform SERS interfaces, narrow plasmon resonance absorption, and strong local electric fields contributing to considerable SERS enhancement[22] in comparison with nonperiodic nanomaterials. These periodic metallic nanostructures provide excellent signal uniformity and reproducibility, as each component exhibits consistent excitation resonance under light

irradiation. Studies have shown that periodic metallic nanostructures deliver a high SERS performance and reduced standard deviation when detecting molecules compared with nonperiodic nanomaterials.[23,24]

In this study, a periodic Ag nanoarray (AgNA) is used as a high-sensitivity SERS substrate in detecting PS nanoparticles within the nanoscale range. The SERS performance of the AgNA is analyzed using R6G molecules as analytes. The localized surface-plasmon-related SERS performance of the AgNA is investigated by optimizing its height. The nonlinear SERS intensity increase ratio under low and high polystyrene nanoplastic (PSNP) concentrations is studied by SEM measurement. The LOD of the proposed AgNA illustrates good sensitivity in detecting PSNPs with an LOD of 10 μg/mL, indicating its good application in detecting PS NPPs with nanoscale diameters.

2. Materials and Methods

2.1 Materials

Hydrogen peroxide solution (H_2O_2, 30%) and ethanol were obtained from Shanghai Aladdin Biochemical Technology Co., Ltd. Nitric acid (HNO_3, 68%) was purchased from Chengdu Chron Chemicals Co. Si wafers were procured from Suzhou Crystal Silicon Electronic & Technology Co., Ltd. Polystyrene (PS) nanoplastics (2.5% w/v in water) were supplied by Shanghai Macklin Biochemical Co., Ltd. Acetone was procured from Chengdu Hualong Chemical Co., Ltd., and anodized aluminum oxide (AAO) was obtained from Shenzhen Tops Precision Film Co., Ltd. All purchased chemicals were used without further purification.

2.2 Preparation of AgNA

A Si substrate (0.8 × 0.8 cm^2) was ultrasonically cleaned at 80 °C for 20 min in a solution of $NH_3 \cdot H_2O$:H_2O_2:H_2O = 1:1:5. After cleaning, the substrate was alternately rinsed three times with deionized water and ethanol for 10 min and then dried with nitrogen gas. The AAO template was soaked in acetone for 10 min to remove the PMMA support film. Afterward, the AAO was transferred onto the Si wafer by a fishing process. The AAO/Si substrate was placed in a desiccator and kept under vacuum for 8 h. Silver atoms were then deposited onto the preprepared samples via thermal evaporation. After the deposition, the AAO template was removed using a tape.

2.3 Sample preparation

A high-concentration PSNP solution with a concentration of 2.5% (w/v) in water was diluted gradually into varying concentrations. For the environmental water condition, tap water was directly used without further treatment. The collected river water and rainwater were first filtered to remove large contaminations. Then, the river water and rainwater were used to prepare the sample.

2.4 SERS experiments

All SERS spectra were obtained using a confocal micro-Raman system (Zolix, Beijing, China) with a 532 nm excitation laser. Measurements were conducted using a 100× objective lens and an 1800 grating. The laser power was set to 1 mW, and the acquisition time was 10 s. The presented SERS spectra represent the average of measurements taken from five randomly selected points on the SERS substrate.

3. Results and Discussion

3.1 Characterization of AgNA

Figure 1(a) shows a brief overview of the fabrication of periodic AgNAs with varying thicknesses. These nanostructures are created by thermally evaporating Ag atoms onto porous

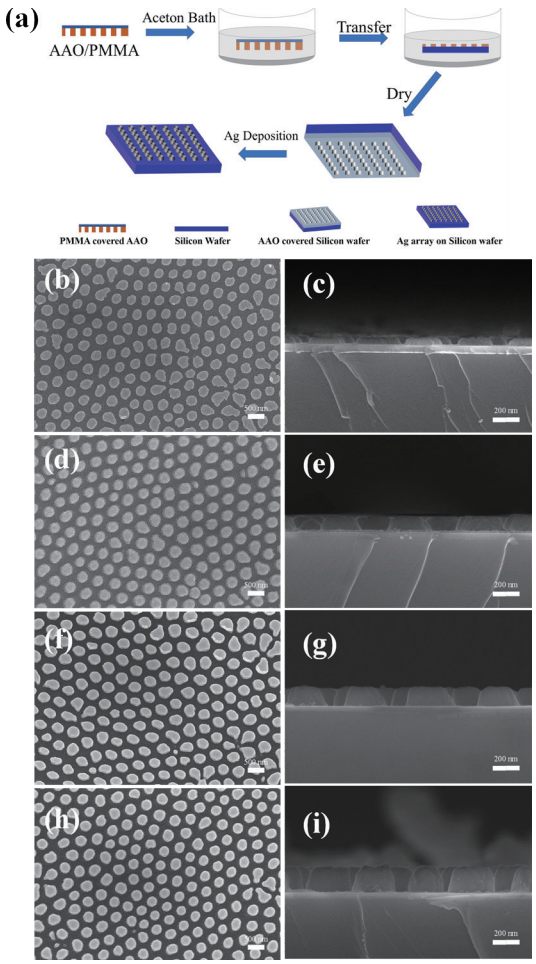

Fig. 1. (Color online) (a) Schematic of AgNA substrate fabrication. Scanned electron microscopy (SEM) images of AgNAs with heights of around (b) 50, (d) 100, (f) 150, and (h) 200 nm. The diameters of the AgNAs are around 260 nm. Corresponding SEM images of cross sections of AgNAs with heights of (c) 50, (e) 100, (g) 150, and (i) 200 nm.

anodic aluminum oxide (AAO) templates. The heights of the AgNAs were controlled by adjusting the deposition time. Scanning electron microscopy (SEM) was used to characterize the resulting AgNA, and the high-resolution SEM images are shown in Fig. 1, which shows that the uniform and periodic structures are clearly visible. Figures 1(b), 1(d), 1(f), and 1(h) show large-scale SEM images of AgNAs fabricated using AAO templates. The measured average diameters of the AgNAs were around 260 nm. Figures 1(c), 1(e), 1(g), and 1(i) are SEM images of cross sections of AgNAs with different heights. By calculation, the corresponding heights are 50, 100, 150, and 200 nm. These results confirm the effectiveness of the proposed method in controlling the AgNA height.

The SERS performance of the proposed AgNAs with varying heights was determined using R6G as an analyte. Figure 2(a) shows the SERS spectra for detecting 10^{-8} M R6G using AgNAs with different heights. The diameter of the AgNAs is 260 nm. By analyzing the intensity of the SERS characteristic peak, the AgNA with a height of 150 nm shows a high SERS performance. Figure 2(b) shows the SERS spectra for detecting R6G with different concentrations using the AgNA with a height of 150 nm. The Raman peak at 613 cm^{-1} corresponds to in-plane C–C–C vibrations in the R6G molecule. The peaks at 775 and 1182 cm^{-1} are associated with out-of-plane

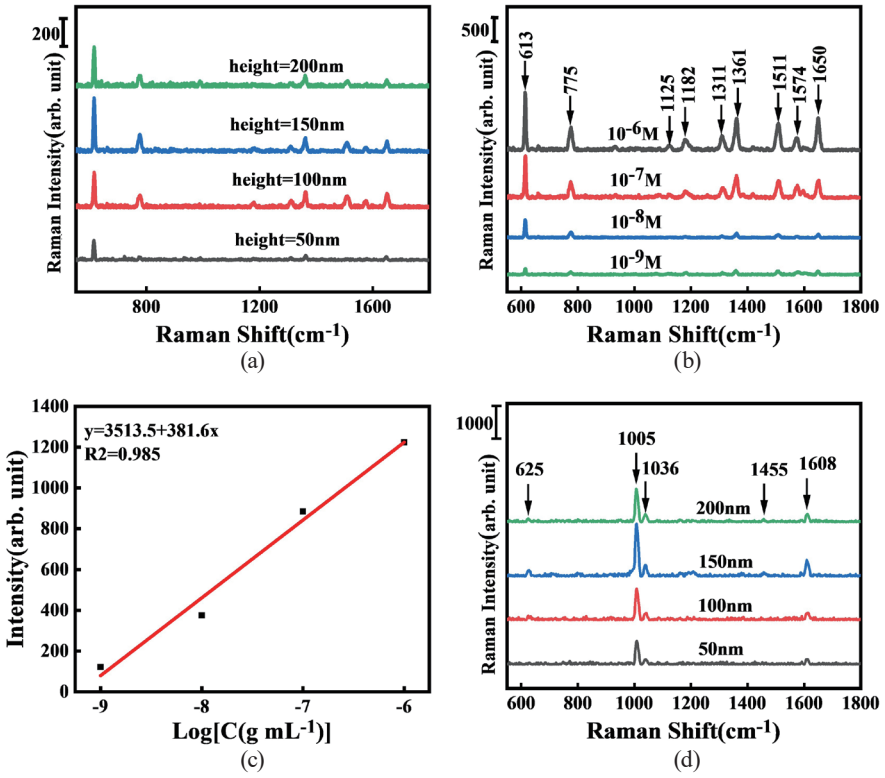

Fig. 2. (Color online) (a) SERS spectra for detecting 10^{-8} M R6G using AgNAs with different heights. The diameter of the AgNAs is 260 nm. (b) SERS spectra for detecting R6G with varying concentrations using optimized AgNA with a diameter of 260 nm and a height of 150 nm. (c) Relationship between R6G concentration and SERS intensity at 613 nm. The fitted curve indicates a linear relationship. (d) SERS spectra for detecting 65-nm-diameter PSNPs using AgNAs with different heights. The diameter of the AgNAs is 260 nm, and the heights are 50, 100, 150, and 200 nm.

and in-plane vibrations of C–H bonds, respectively. Additionally, the peaks observed at 1311, 1361, 1511, and 1650 cm^{-1} can be attributed to aromatic C–C stretching vibrations. Figure 2(c) shows the characteristic peak intensities of R6G at 613 cm^{-1} across different concentrations, and it also shows a linear relationship. By observation, the LOD of AgNAs in detecting R6G is 10^{-9} M. These results demonstrate the effectiveness of the proposed AgNA substrates for quantitative analysis. Figure 2(d) shows the SERS spectra for detecting 65-nm-diameter PSNPs on AgNAs with heights of 50 50, 100, 150, and 200 nm. The characteristic Raman peaks at 625, 1005, 1036, and 1608 cm^{-1} correspond to the C–C–O stretching, ring breathing, C–H in-plane deformation, and ring skeletal stretching modes of the PSNPs, respectively. When the PSNP concentration is 0 μg/mL, no SERS peaks are observed. With increasing height of the AgNA, the SERS performance of the AgNA increases and then decreases. By analyzing the intensity of the SERS characteristic peak, the AgNA with a height of 150 nm shows a higher SERS performance.

3.2 Detection of PSNPs with different concentrations

Figures 3(a) and 3(c) show the SEM images of the PSNPs used. The size distribution of the PSNPs is presented in Figs. 3(b) and 3(d). By calculation, the average sizes of the PSNPs in Figs. 3(a) and 3(c) are around 65 and 448 nm, respectively. Figures 3(e) and 3(g) are the SEM images of PSNPs with diameters of 65 and 488 nm, respectively, on the AgNA with a diameter of 260 nm and a height of 150 nm. By observation, the 65-nm-diameter PSNPs are connected to the AgNA, whereas the 448-nm-diameter PSNPs are suspended at the top of the AgNA. Figures 3(f) and 3(h) show the SERS spectra for detecting PSNPs with diameters of 65 and 488 nm, respectively, at varying concentrations. Notably, at a PSNP concentration of 0 μg/mL, no SERS peaks are observed. As the concentration of PSNPs increases, the SERS intensity correspondingly rises. In Figs. 3(f) and 3(h), the intensity of the SERS characteristic peak at 1005 cm^{-1} belonging to PSNPs increases with the concentration of PSNPs. However, the characteristic peak intensity increase ratio from 10 to 100 μg/mL is larger than the change in the concentration from 100 to 500 μg/mL. This phenomenon can be explained by the aggregation of the PSNPs at high concentrations. Figures 4(a) and 4(b) are the SEM images of the 65-nm-diameter PSNPs with concentrations of 10 and 500 μg/mL, respectively. At lower concentrations of PSNPs, the PSNPs connect with the AgNA, causing a highly enhanced SERS intensity per unit mass. At higher concentrations, some of the PSNPs do not come in contact with the AgNA and are located between the AgNAs, resulting in a lower enhanced SERS intensity per unit mass. Thus, this phenomenon caused a nonlinear SERS performance. Moreover, in this experiment, the PSNPPs are diluted from high concentration to low concentration gradually. The PSNPs with a concentration lower than 10 μg/mL have been tested and there is no SERS signal detected. Thus, the LOD of our proposed AgNA is 10 μg/mL.

Table 1 shows a comparative assessment of the analytical performance of the proposed SERS method alongside other SERS-based techniques for PSNP analysis. The PSNPs are detected through a wide range of diameters from 20 to 800 nm. The Au nanopore,[25] AuNSs@Ag@AAO,[26] commercially available Klarite substrates,[27] and AgNW arrays[28] have been used for detecting PSNPs with an LOD ranging from 50 to 500 μg/mL. The AgNA proposed in this study illustrates a lower LOD of 10 μg/mL, indicating its good detection performance.

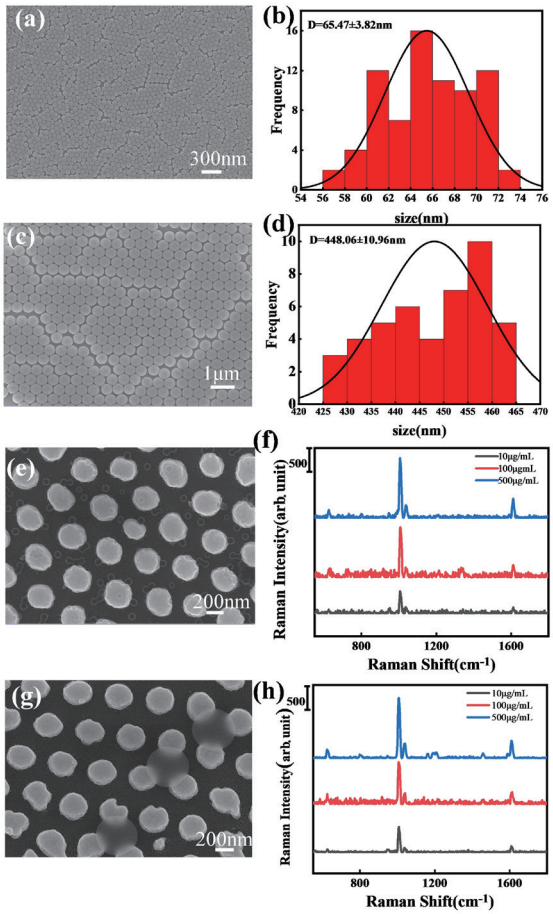

Fig. 3. (Color online) (a) and (c) SEM images of PSNPs with diameters of 65 and 448 nm, respectively. (b) and (d) Size distributions of PSNPs. (e) and (g) SEM images of PSNPs with diameters of 65 and 488 nm, respectively, on AgNA with a diameter of 260 nm and a height of 150 nm. (f) and (h) Corresponding SERS spectra of PSNPs with different concentrations obtained from AgNA. The concentrations of PSNPs are 10, 100, and 500 μg/mL.

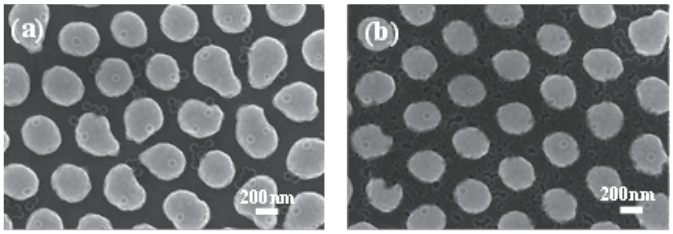

Fig. 4. (Color online) SEM images of PSNPs with concentrations of (a) 10 and (b) 500 μg/mL.

Table 1
Comparable results of varying SERS substrates in detecting PSNPs.

SERS substrates	PSNP size (nm)	LOD (μg/mL)	Reference
Au nanopore	20	500	25
AuNSs@Ag@AAO	400	50	26
Klarite	360	100	27
AgNW arrays	630	100	28
AgNA	70	10	This work

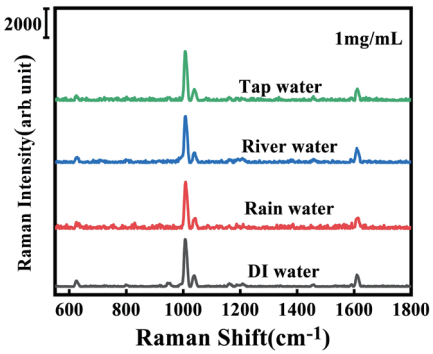

Fig. 5. (Color online) Spectra of detected PSNPs under real water conditions (tap water, river water, rainwater, and deionized water).

Table 2
Detection of PSNPs under different water conditions by the proposed method.

Samples	Spiked (mg/mL)	Total found (mg/mL)	Recovery ratio (%)	RSD (%)
Tap water	1	0.97	97	8.7
River water	1	0.95	95	9.2
Rainwater	1	0.95	95	10.1

3.3 Detection of PSNPs under environmental water conditions

The proposed AgNA is applied to detect 65-nm-diameter PSNPs with a concentration of 1 mg/mL under varying water conditions. Figure 5 shows the SERS spectra for detecting 65-nm-diameter PSNPs with a concentration of 1 mg/mL in tap water, river water, rainwater, and deionized water. Figure 5 reveals that the appearance of the characteristic peaks of the PSNPs proves their successful detection. Table 2 shows the recovery rate of the proposed AgNA in detecting PSNPs under different water conditions in which the characteristic peak at 1005 cm^{-1} is selected to calculate the concentration of the PSNPs. The calculated recovery ratio is around 95.6% and the RSD is around 9.3%.

4. Conclusions

In this study, we developed a simple and effective method for the quantitative analysis of PSNPs in nanoscale ranges. The easily fabricated AgNA, which serves as the SERS substrate, was produced by thermally depositing Ag onto AAO templates. The SERS performance mechanism of the AgNA substrate was investigated by changing its height. The AgNA substrate successfully detected PSNPs and the LOD was 10 μg/mL. Compared with the reported substrates for analyzing PSNPs, this SERS substrate demonstrated high sensitivity and directly detected PSNPs without the need for pretreatment or chemical additives. The good recovery rate and RSD proved the practical application of the proposed AgNA. This straightforward and efficient SERS substrate opens up new possibilities for the rapid detection of NPPs in the water environment.

Acknowledgments

This work was supported by the National Key Research and Development Program of China (No. 2022YFE0134600), Guangxi Science and Technology Project (No. AD22035215), Guangxi Natural Science Foundation Project (No. 2021GXNSFBA196049), the National Key Research and Development Program of China (No. 2021YFA0715404), and the Key Research and Development Program of Guangxi (No. AB22080055).

References

1 J. Zhang, M. Peng, E. Lian, L. Xia, A. G. Asimakopoulos, S. Luo, and L. Wang: Environ. Sci. Technol. **57** (2023) 8365. https://doi.org/10.1021/acs.est.3c00842
2 K. Zhang, X. Xiong, H. Hu, C. Wu, Y. Bi, Y. Wu, B. Zhou, P. K. S. Lam, and J. Liu: Environ. Sci. Technol. **51** (2017) 3794. https://doi.org/10.1021/acs.est.7b00369
3 J. Ding, F. Jiang, J. Li, Z. Wang, C. Sun, Z. Wang, L. Fu, N. X. Ding, and C. He: Environ. Sci. Technol. **53** (2019) 8036. https://doi.org/10.1021/acs.est.9b01452
4 D. Yang, H. Shi, L. Li, J. Li, K. Jabeen, and P. Kolandhasamy: Environ. Sci. Technol. **49** (2015) 13622. https://doi.org/10.1021/acs.est.5b03163
5 H. A. Leslie, M. J. Van Velzen, S. H. Brandsma, A. D. Vethaak, J. J. Garcia-Vallejo, and M. H. Lamoree: Environ. Int. **163** (2022) 107199. https://doi.org/10.1016/j.envint.2022.107199
6 T. Ishimura, I. Iwai, K. Matsui, M. Mattonai, A. Watanabe, W. Robberson, A.-M. Cook, H. L. Allen, W. Pipkin, N. Teramae, H. Ohtani, and C. Watanabe: J. Anal. Appl. Pyrolysis **157** (2021) 105188. https://doi.org/10.1016/j.jaap.2021.105188
7 C. F. Araujo, M. M. Nolasco, A. M. P. Ribeiro, and P. J. A. Ribeiro-Claro: Water Res. **142** (2018) 426. https://doi.org/10.1016/j.watres.2018.05.060
8 M. M.-L. Leung, Y.-W. Ho, C.-H. Lee, Y. Wang, M. Hu, K. W. H. Kwok, S.-L. Chua, and J. K.-H. Fang: Environ. Pollut. **289** (2021) 117648. https://doi.org/10.1016/j.envpol.2021.117648
9 R. Lenz, K. Enders, C. A. Stedmon, D. M. A. Mackenzie, and T. G. Nielsen: Mar. Pollut. Bull. **100** (2015) 82. https://doi.org/10.1016/j.marpolbul.2015.09.026
10 A. Käppler, D. Fischer, S. Oberbeckmann, G. Schernewski, M. Labrenz, K.-J. Eichhorn, and B. Voit: Anal. Bioanal. Chem. **408** (2016) 8377. https://doi.org/10.1007/s00216-016-9956-3
11 J.-L. Xu, K. V. Thomas, Z. Luo, and A. A. Gowen: TrAC, Trends Anal. Chem. **119** (2019) 115629. https://doi.org/10.1016/j.trac.2019.115629
12 D. Materić, A. Kasper-Giebl, D. Kau, M. Anten, M. Greilinger, E. Ludewig, E. van Sebille, T. Röckmann, and R. Holzinger: Environ. Sci. Technol. **54** (2020) 2353. https://doi.org/10.1021/acs.est.9b07540
13 A. Barber, S. Kly, M. G. Moffitt, L. Rand, and J. F. Ranville: Environ. Sci.: Nano **7** (2020) 514. https://doi.org/10.1039/C9EN00637K
14 J. Jiménez-Lamana, L. Marigliano, J. Allouche, B. Grassl, J. Szpunar, and S. Reynaud: Anal. Chem. **92** (2020) 11664. https://doi.org/10.1021/acs.analchem.0c01536
15 P. Mao, C. Liu, G. Favraud, Q. Chen, M. Han, A. Fratalocchi, and S. Zhang: Nat. Commun. **9** (2018) 5428. https://doi.org/10.1038/s41467-018-07869-5
16 Y. Liu and F. Luo: Nano Res. **13** (2020) 138. https://doi.org/10.1007/s12274-019-2586-2
17 G. Xu, H. Cheng, R. Jones, Y. Feng, K. Gong, K. Li, X. Fang, M. A. Tahir, V. K. Valev, and L. Zhang: Environ. Sci. Technol. **54** (2020) 15594. https://doi.org/10.1021/acs.est.0c02317
18 Y. Liu, Z. Qin, X. Jia, J. Zhou, H. Li, X. Wang, and G. Wang: J. Environ. Chem. Eng. **12** (2024) 113311. https://doi.org/10.1016/j.jece.2024.113311
19 J. Li, H. Liu, S. Chen, X. Liang, Y. Gao, X. Zhao, Z. Li, C. Zhang, F. Lei, and J. Yu: J. Phys. Chem. Lett. **13** (2022) 5815. https://doi.org/10.1021/acs.jpclett.2c01534
20 J. Caldwell, P. Taladriz-Blanco, B. Rothen-Rutishauser, and A. Petri-Fink: Nanomaterials **11** (2021) 1149. https://doi.org/10.3390/nano11051149
21 R. Hu, K. Zhang, W. Wang, L. Wei, and Y. Lai: J. Hazard. Mater. **429** (2022) 128388. https://doi.org/10.1016/j.jhazmat.2022.128388
22 Y. Liu, J. Deng, Z. Jin, T. Liu, J. Zhou, F. Luo, and G. Wang: Nano Res. **15** (2022) 6062. https://doi.org/10.1007/s12274-022-4310-x

23 K.-H. Chen, M.-J. Pan, Z. Jargalsaikhan, T.-O. Ishdorj, and F.-G. Tseng: Biosensors **10** (2020) 163. https://doi.org/10.3390/bios10110163
24 M. J. Bistaffa, S. A. Camacho, W. M. Pazin, C. J. L. Constantino, O. N. Oliveira, Jr., and P. H. B. Aoki: Talanta **244** (2022) 123381. https://doi.org/10.1016/j.talanta.2022.123381
25 X.-L. Nie, H.-L. Liu, Z.-Q. Pan, S. A. Ahmed, Q. Shen, J.-M. Yang, J.-B. Pan, J. Pang, C.-Y. Li, X.-H. Xia, and K. Wang: Chem. Commun. **55** (2019) 6397. https://doi.org/10.1039/c9cc01358j
26 Q. T. Lê, N. H. Ly, M.-K. Kim, S. H. Lim, S. J. Son, K.-D. Zoh, and S.-W. Joo: J. Hazard. Mater. **402** (2021) 123499. https://doi.org/10.1016/j.jhazmat.2020.123499
27 G. Xu, H. Cheng, R. Jones, Y. Feng, K. Gong, K. Li, X. Fang, M. A. Tahir, V. K. Valev, and L. Zhang: Environ. Sci. Technol. **54** (2020) 15594. https://doi.org/10.1021/acs.est.0c02317
28 Y. Jeon, D. Kim, G. Kwon, K. Lee, C.-S. Oh, U.-J. Kim, and J. You: Carbohydr. Polym. **272** (2021) 118470. https://doi.org/10.1016/j.carbpol.2021.118470